J. Fluid Mech. (1967), *vol.* 30, *part* 3, *pp.* 465–478
Printed in Great Britain

Convection in a box: linear theory

By STEPHEN H. DAVIS
The RAND Corporation, Santa Monica, California†

(Received 2 May 1967)

The linear stability of a quiescent, three-dimensional rectangular box of fluid heated from below is considered. It is found that finite rolls (cells with two non-zero velocity components dependent on all three spatial variables) with axes parallel to the shorter side are predicted. When the depth is the shortest dimension, the cross-sections of these finite rolls are near-square, but otherwise (in wafer-shaped boxes) narrower cells appear. The value of the critical Rayleigh number and preferred wave-number (number of finite rolls) for a given size box is determined for boxes with horizontal dimensions h, $\frac{1}{4} \leqslant h/d \leqslant 6$, where d is the depth.

1. Introduction

There has been much recent interest in the understanding of cellular convection. In particular, much of this work has been directed toward the prediction of the preferred mode (cell shape) of convective cells after the onset of convection (Segel & Stuart 1962; Schlüter, Lortz & Busse 1965). The model generally used consists of a thin, horizontal fluid layer, infinite in horizontal extent and heated from below. The analyses of the governing equations aim at resolving the doubly infinitely degenerate spectrum of wave-numbers, which is allowable by the linearized equations, into a preferred one (only one appears to be present in experiments) through non-linear selection. It seems, however, as though these theories are not comparable with experiments, since the necessary lateral confining walls make their presence felt by not allowing non-linear selection to manifest itself by the array of hexagonal cells predicted (in an interval about the critical Rayleigh number) by the non-linear theories. These predictions of hexagons depend on any of several small parameters such as measures of fluid property variation with temperature and deflexion of free surfaces (Davis & Segel 1965). Instead, roll cells of geometrical shape similar to that of the confining container seem to appear (Koschmieder 1966) in the right circular cylinder and the rectangular parallelpiped, the influence of the lateral boundaries dominating over the small aforementioned effects.

The purpose of this study is to determine the influence of lateral walls on the convective process in a rectangular box (cylinder). Previous attention to this problem has been paid by Pellew & Southwell (1940), Zierep (1963), and Ostrach

† Present address: Department of Mathematics, Imperial College, London S.W.7, England.

& Pnueli (1963). Zierep and Pellew & Southwell recognized that the presence of rigid lateral walls makes separation of variables impossible (all of the boundary conditions on the vertical walls cannot be satisfied), and so they considered idealized 'slip walls'. Ostrach & Pnueli obtained a sixth-order linear partial differential for the vertical velocity w with the boundary conditions $w = \partial w/\partial z = \Delta^2 w = 0$ on all boundaries. On vertical walls, however, the condition $\partial w/\partial z = 0$ is redundant, while no heed was taken of the fact that the horizontal velocity components must also vanish there. Separation of variables was used to obtain critical Rayleigh numbers which are insensitive to these latter conditions. Hence Ostrach & Pnueli's numbers are incorrect and predictably lie between $R_c = 1708$, the value for the infinite layer, and our results, where the boundary conditions are correct and hence more severely restrict the eigenfunctions.

It is to be expected that since the linear stability problem is to be solved in a closed and bounded domain, the spectrum of allowable wave-numbers will be denumerable corresponding to multiples of the horizontal dimensions. A Galerkin procedure is used to obtain approximate critical Rayleigh numbers (upper bounds) whose corresponding approximate eigenfunctions satisfy all boundary conditions and continuity exactly. This last condition ensures that implicit boundary conditions such as $\partial w/\partial z = 0$ on horizontal boundaries are satisfied.

The results obtained for boxes with width to depth ratios h/d in the range $\frac{1}{4} \leqslant h/d \leqslant 6$ are the following.

(i) The preferred mode is always some number of finite rolls (two non-zero velocity components dependent on three spatial variables) with axes parallel to the short side (square boxes excepted).

(ii) When the depth is the smallest dimension, finite rolls of near-square cross-section are predicted. Otherwise narrower finite rolls appear.

(iii) The critical Rayleigh number decreases rapidly to the value 1708 as the horizontal dimensions increase so that most experiments, which use thin layers, would appear to have onset occur at about $R_c = 1708$.

(iv) A diagram (figure 13) is presented which makes it possible, when the horizontal dimensions of the box are known, to determine R_c and the preferred mode according to linear theory.

2. Formulation of the problem

We shall use the following notation and dimensionless variables: d is the distance between the horizontal boundaries of a rectangular box which encloses a fluid of mean density ρ_0; g is the acceleration of gravity (taken to act vertically downward); and α, ν and κ are the constant coefficients of thermal expansion, kinematic viscosity and thermal diffusivity, respectively. The dimensionless horizontal co-ordinates x and y, respective horizontal dimensions h_1 and h_2, and vertical co-ordinate z refer to the length d. The velocity $\mathbf{V} = (u, v, w)$, temperature T, time t and pressure p refer to the scales $q_0 = [\alpha(\Delta T)\ gd\kappa/\nu]^{\frac{1}{2}}$, ΔT, d^2/κ and $\rho_0 \nu q_0/d$, respectively. Here ΔT is the temperature difference between top and bottom. We use the Boussinesq approximation. The linear equations that govern an infinitesimal disturbance of the initial quiescent layers with temperature

profile $\overline{T} = -z$ are as follows (see Davis & Segel 1965, equations (2.9)–(2.12) with $\gamma = \delta = \zeta = 0$ and non-linear terms neglected):

$$\operatorname{div} \mathbf{V} = 0, \tag{2.1}$$

$$\left(P^{-1}\frac{\partial}{\partial t} - \Delta\right)\mathbf{V} - R^{\frac{1}{2}}\theta\mathbf{k} + \operatorname{grad} p = 0, \tag{2.2}$$

$$\left(\frac{\partial}{\partial t} - \Delta\right)\theta - R^{\frac{1}{2}}w = 0. \tag{2.3}$$

Here $$\Delta = \frac{\partial^2}{\partial x^2} + \frac{\partial^2}{\partial y^2} + \frac{\partial^2}{\partial z^2};$$

P is the Prandtl number ν/κ; R is the Rayleigh number $\alpha(\Delta T)gd^3/\kappa\nu$, which is assumed positive (the fluid is 'heated from below'); θ is the deviation from the mean temperature $\overline{T}$; and $\mathbf{k} = (0, 0, 1)$.

The boundaries are all considered to be rigid and perfect heat conductors so that

$$\mathbf{V} = \theta = 0 \quad \text{on} \quad |z| = \tfrac{1}{2}, \quad |x| = \tfrac{1}{2}h_1, \quad |y| = \tfrac{1}{2}h_2. \tag{2.4}$$

Equations (2.2) and (2.3) can be written in terms of a matrix operator D, which is defined by

$$D = \begin{bmatrix} \Delta & R^{\frac{1}{2}}\mathbf{k} \\ R^{\frac{1}{2}}\mathbf{k} & \Delta \end{bmatrix}, \tag{2.5}$$

as

$$-\frac{\partial}{\partial t}\begin{bmatrix} P^{-1}\mathbf{V} \\ \theta \end{bmatrix} + D.\begin{bmatrix} \mathbf{V} \\ \theta \end{bmatrix} - \begin{bmatrix} \operatorname{grad} p \\ 0 \end{bmatrix} = \begin{bmatrix} 0 \\ 0 \end{bmatrix}, \tag{2.6a}$$

$$\operatorname{div} \mathbf{V} = 0. \tag{2.6b}$$

One advantage of writing the governing equations in this way is derived from the fact that D is self-adjoint using the boundary conditions (2.4) and equation (2.6b). That is

$$\begin{aligned} \langle \tilde{\Psi}.(D.\Psi)\rangle &= \langle \tilde{\mathbf{V}}.\Delta\mathbf{V} + R^{\frac{1}{2}}(\tilde{w}\theta + w\tilde{\theta}) + \tilde{\theta}\Delta\theta\rangle \\ &= \langle \Delta\tilde{\mathbf{V}}.\mathbf{V} + R^{\frac{1}{2}}(\tilde{w}\theta + w\tilde{\theta}) + (\Delta\tilde{\theta})\theta\rangle \\ &= \langle (D.\tilde{\Psi}).\Psi\rangle. \end{aligned}$$

Here $\Psi \equiv (u, v, w, \theta)$, and the inner product of two functions a and b is defined by

$$\langle ab\rangle \equiv \int_{-\frac{1}{2}}^{\frac{1}{2}}\int_{-\frac{1}{2}h_2}^{\frac{1}{2}h_2}\int_{-\frac{1}{2}h_1}^{\frac{1}{2}h_1} ab\,dx\,dy\,dz.$$

This self-adjointness guarantees that the stability boundary (marginal stability) is characterized by non-oscillatory motions (Sani 1963) (the principle of exchange of stabilities). The onset of convection is thus governed by the following equations:

$$D.\Psi - \begin{bmatrix} \operatorname{grad} p \\ 0 \end{bmatrix} = \begin{bmatrix} 0 \\ 0 \end{bmatrix}, \tag{2.7a}$$

$$\operatorname{div} \mathbf{V} = 0 \tag{2.7b}$$

with the boundary conditions (2.4).

In general the system (2.7) is non-separable. An approximate solution may be obtained using the Galerkin procedure.

3. Galerkin procedure

Let us consider a complete space $\mathscr{S}$ of trial functions containing the following sets:

$\mathscr{S}_1 = \{\psi_n(\mathbf{x})\}$, a set of scalar functions whose elements have continuous first and second partial derivatives with respect to x, y, z, and $\psi_n(\mathbf{x}) = 0$ on the boundary.

$\mathscr{S}_2 = \{\boldsymbol{\phi}_n(\mathbf{x})\}$, a set of vector functions $\boldsymbol{\phi}_n = (\phi_n^{(1)}, \phi_n^{(2)}, \phi_n^{(3)})$, whose elements have continuous first and second partial derivatives with respect to x, y, z. $\operatorname{div}\boldsymbol{\phi}_n = 0$ and $\boldsymbol{\phi}_n(\mathbf{x}) = 0$ on the boundary.

$\mathscr{S}_3 = \{p_n(\mathbf{x})\}$, a set of scalar functions whose elements have continuous first partial derivatives with respect to x, y, z.

An important consequence of the requirement $\operatorname{div}\boldsymbol{\phi}_n = 0$ is that on all boundaries of the box, the *implicit* condition that the normal derivative of the component of velocity normal to the boundaries is zero, is satisfied. For example, on a boundary defined by $x = \pm \frac{1}{2}h_1$, $\partial/\partial y = \partial/\partial z$ are tangential derivatives. Thus, the continuity condition implies that $\partial/\partial x \phi_n^{(1)} = 0$ on boundaries where $x = \pm \frac{1}{2}h_1$. Similarly, both the conditions, $\partial/\partial y \phi_n^{(2)} = 0$ on boundaries where $y = \pm \frac{1}{2}h_2$, and $\partial/\partial z \phi_n^{(3)} = 0$ on horizontal boundaries, are exactly satisfied. In addition, if continuity were not satisfied exactly, the following approximate procedure would not necessarily yield upper bounds, nor would convergence be guaranteed. Let us represent $\mathbf{V}$, θ and p as follows:

$$\mathbf{V} = \sum_{n=1}^{\infty} c_n \boldsymbol{\phi}_n,$$

$$\theta = \sum_{n=1}^{\infty} d_n \psi_n,$$

$$p = \sum_{n=1}^{\infty} e_n p_n.$$

We shall substitute the first N terms of these into equation (2.7). As this is not an exact solution, there will be an error. We require that this error be orthogonal to each four-vector

$$\begin{bmatrix} \boldsymbol{\phi}_j \\ \psi_j \end{bmatrix}$$

and obtain the linear algebraic equations:

$$\left.\begin{aligned} \sum_{i=1}^{N} (d_i \langle \psi_k \Delta \psi_i \rangle + R^{\frac{1}{2}} c_i \langle \phi_i^{(3)} \phi_k \rangle) = 0 \qquad (k = 1, 2, \ldots, N), \\ \sum_{i=1}^{N} (R^{\frac{1}{2}} d_1 \langle \psi_i \phi_k^{(3)} \rangle + c_i \langle \boldsymbol{\phi}_k . \Delta \boldsymbol{\phi}_i \rangle) = 0 \qquad (k = 1, 2, \ldots, N). \end{aligned}\right\} \tag{3.1}$$

The pressure term vanishes by virtue of the facts that $\operatorname{div}\boldsymbol{\phi}_i = 0$ and $\boldsymbol{\phi}_i$ is zero on the boundary. Equations (3.1) have non-trivial solutions if and only if

$$\det \begin{bmatrix} U & R^{\frac{1}{2}} V \\ R^{\frac{1}{2}} W & Z \end{bmatrix} \equiv \det A = 0,$$

where U, V, W, Z are $N \times N$ matrices defined as follows:

$$U = -(\langle \nabla\psi_i . \nabla\psi_k \rangle),$$

$$V = (\langle \phi_i^{(3)} \psi_k \rangle),$$

$$W = (\langle \phi_k^{(3)} \psi_i \rangle),$$

$$Z = -(\langle \nabla\phi_i^{(1)} . \nabla\phi_k^{(1)} + \nabla\phi_i^{(2)} . \nabla\phi_k^{(2)} + \nabla\phi_i^{(3)} . \nabla\phi_k^{(3)} \rangle).$$

Simplification of U and Z has been obtained by using integration by parts and the boundary conditions (2.4). The critical Rayleigh number R_c is the smallest positive value of R for which $\det A = 0$ as $N \to \infty$ (see appendix A for details of computation).

It is worth noting that the Galerkin procedure being used is equivalent to a Rayleigh–Ritz procedure using the following maximum principle due to Sani (1963):

$$R_c^{-\frac{1}{2}} = \max_{\mathscr{S}} \frac{2\langle \theta w \rangle}{\langle \nabla u . \nabla u + \nabla v . \nabla v + \nabla w . \nabla w + \nabla\theta . \nabla\theta \rangle} \tag{3.2}$$

with $$\operatorname{div} \mathbf{V} = 0.$$

The equivalence is due to the self-adjointness of D. Consequently, we expect that as we increase N (the number of terms in the Galerkin approximation), the upper bound of R_c will decrease monotonically and converge to the exact R_c of (2.7).

One point concerning our approach should be emphasized. By using the full system of equations rather than a higher order equation obtained by cross-differentiation and elimination, our trial functions need have only two derivatives close to the exact solution. This should promote rapid convergence.

Finite roll approximation

In the problem of a heated infinite horizontal fluid layer, linear theory fixes the critical overall wave-number but does not otherwise distinguish the x–y dependence of the eigensolution. The linear problem may thus be solved in the simplest case, the roll cell. A general solution can then be obtained by superposition. A roll is a cell with only two non-zero velocity components dependent upon two spatial variables, uniform and of infinite extent in the third direction. With a fully enclosed geometry, we can define *finite rolls* which have only *two non-zero velocity components* but by necessity are *dependent upon* all *three spatial variables*. This dependence guarantees that all boundary conditions can be satisfied. We will term a finite roll a *finite x-roll* when its *axes* are *parallel* to the *y-axis* (zero y component of velocity) and similarly a *finite y-roll* is one whose *axis* is *parallel* to the *x-axis*. As a first step, we shall consider trial functions which have the properties of finite rolls. (For a discussion of the physical possibility of having a flow with only two non-zero velocity components existing in a fully confined domain, see § 5.) All trial functions must satisfy the boundary conditions and the continuity equation exactly. For the construction of any number of finite x-rolls and finite y-rolls, refer to appendix B.

Let us fix our attention on K finite y-rolls with regard to the dependence of R_c upon (h_1, h_2). Two types of behaviour become apparent.

Type I. Let us fix h_1 and allow h_2 to vary for K finite y-rolls. A typical stability curve is shown in figure 1. The shape is qualitatively similar to the stability curve for the infinite layer in that there is a minimum at a finite value of h_2.

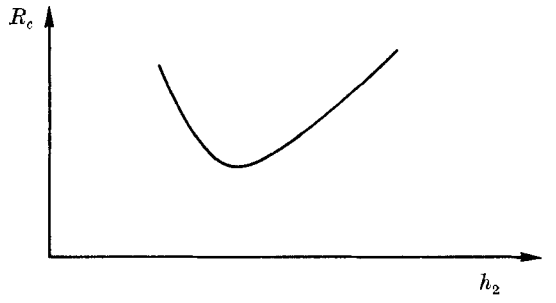

FIGURE 1. Qualitative behaviour of K finites y-rolls, R_c versus h_2 with h_1 fixed; type I dependence.

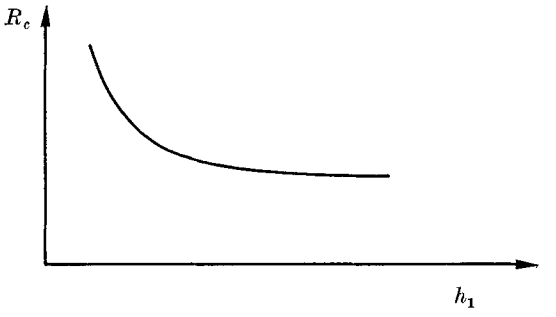

FIGURE 2. Qualitative behaviour of K finites y-rolls, R_c versus h_1 with h_2 fixed; type II dependence.

Type II. Let us fix h_2 and allow h_1 to vary for K finite y-rolls. A typical stability curve is shown in figure 2. The curve is monotone decreasing and very rapidly approaches a positive value as $h_1 \to \infty$.

These behaviours will be discussed on physical grounds in §5.

Our criterion for numerical convergence is that if the addition of five consecutive trial functions decreases the approximate R_c by less than 1%, we terminate. We have found that $N = 10$ is sufficient in all cases examined.

Using the fact that $R_c(\alpha, \beta)$ for K finite x-rolls equals $R_c(\beta, \alpha)$ for K finite y-rolls (they are identical physically), we can construct stability curves for the box as follows. Let us fix h_1, say, near $h_1 = 1$. Let us approximate K finite y-rolls and compute R_c as a function of h_2 for $K = 1, 2, 3, \ldots$ Each curve is qualitatively similar to that in figure 1 but as K increases, the minima lie below and to the right of those with smaller K. These curves are denoted by $1y$, $2y$, etc., in figure 3. Let us now construct K finite x-rolls and compute their stability curves. Figure 2 illustrates typical behaviour for each K. When $K = 1$ and $h_2 < h_1$, the resulting curve has a negative slope of smaller magnitude than that for one finite y-roll.

Since the computed R_c's for both cases must be equal when $h_1 = h_2$ (the same physical situation), one finite x-roll is preferable (has a lower R_c) to one finite y-roll when $h_2 < h_1$. In analogous fashion, as finite x-rolls with $K = 2, 3, \ldots$ are considered, curves with negative slopes of smaller magnitude but with larger asymptotes for large h_2 (i.e. displaced upwards), are encountered as K increases. These are labelled $1x$, $2x$, etc., in figure 3. As h_2 is decreased further, finite x-rolls

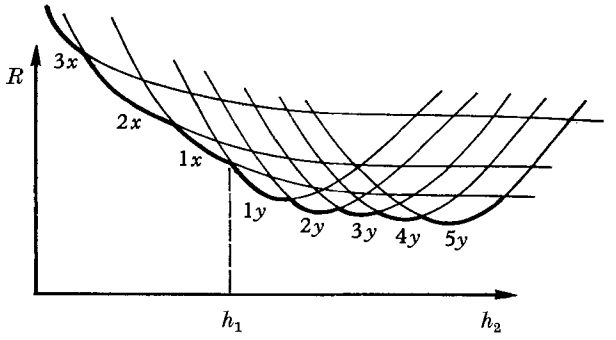

FIGURE 3. Qualitative behaviour of composite stability curve with h_1 fixed. R_c versus h_2, n_x and m_y denote n finite x-rolls and m finite y-rolls respectively. The darkened portion is the minimum critical Rayleigh number.

with larger K (flatter curves which are higher at large h_2), intersect and become the lowest of the curves for an interval of h_2. These x-rolls in turn yield to x-rolls with larger K for smaller h_2. That curve, which consists at h_2 of the lowest permissible value of R_c of all these curves, is the *curve of the critical Rayleigh number* for that h_1. In figure 3, this curve is darkened. This procedure has been used to construct appropriate stability curves for various fixed h_1's. These stability curves are given in figures 4–12. These differ from one another qualitatively in the following way. When h_1 is sufficiently large (approximately greater than 1·75), one finite roll is never preferred and the lowest K allowable is $K = 2$. Similarly, when $h_1 > 2{\cdot}9$, $K = 3$ is the smallest allowable K. These situations are clearly shown in figure 13.

Remark. For h_1 fixed and h_2 sufficiently large, the curve for K finite x-rolls clearly falls below that for K finite y-rolls. For $h_2 > h_1$, however, this curve is always above that for K finite y-rolls for various other K's. For $h_2 < h_1$, the reverse is true; K finite x-rolls for some K always have stability curves below those for any number of finite y-rolls. This is the reason we predict finite rolls with axes parallel to the shorter side of the box.

More general approximations

Let us now consider trial functions which approximate general three-dimensional flows rather than merely finite rolls. An arbitrary one is $\Psi = (u, v, w, \theta)$ with $u_x + v_y + w_z = 0$. A function Ω can be found such that $\Psi_1 = (u, 0, \Omega, \theta_1)$, $\Psi_2 = (0, v, w - \Omega, \theta_2)$ with $u_x + \Omega_z = 0$ and $\theta_1 + \theta_2 = \theta$, and all boundary conditions are satisfied. Clearly, $\Psi_1 + \Psi_2 = \Psi$ and both $(u, 0, \Omega)$ and $(0, v, w - \Omega)$ are divergence-free. *Thus, a general approximate solution can be written as a sum of two approximate finite rolls.*

Our problem has been reduced to the superpositions of finite rolls. Consider the approximate solution $\Psi = \alpha_1\Psi_1 + \alpha_2\Psi_2$ where Ψ_1 and Ψ_2 are finite rolls. Let R_{c_1} be the R_c obtained by letting $\Psi = \Psi_1$ and R_{c_2} be that R_c when $\Psi = \Psi_2$. The *approximation scheme selects* $R_c = R_{c_1}$ and $\alpha_1 = 0$ if $R_{c_1} > R_{c_2}$ or it selects $R_c = R_{c_2}$ and $\alpha_2 = 0$ if $R_{c_2} > R_{c_1}$ (within numerical accuracy). *No mixture is possible* unless $R_{c_1} = R_{c_2}$ in which case finite amplitude effects make the selections. We thus may consider finite rolls individually (as we did in the last section) and obtain results for the full three-dimensional problem.

4. Results

A check of our numerical results is possible. Velte (1964) has computed R_c using a finite difference and variational technique for the case of a two-dimensional channel. For a channel of square cross-section he obtained $R_c = 5030$ in association with a single (not finite) roll. A single finite x-roll with $h_1 = 1$ and h_2 large would be a proper comparison. When $h_2 = 10$ instead of infinity, we get $R_c = 5035$. Since with h_1 fixed and h_2 varying a finite x-roll displays the type II dependence (monotone decreasing), when $h_2 \to \infty$, the two results agree quite closely. Stability curves for h_1 constant, i.e. $R_c(h_1, h_2)$ versus h_2, are shown in figures 4–12. Figure 3 shows schematically that when $h_1 \sim 1$ and h_2 is increased beyond $h_2 = h_1$, finite y-rolls are preferred first with $K = 1$, and then with subsequent transition to $K = 2$, $K = 3$, etc. When h_2 is decreased below $h_2 = 1$, finite x-rolls are preferred again first with $K = 1$, then $K = 2$, etc. In the special case $h_1 = h_2$, any linear combination of one finite x-roll with one finite y-roll is allowable. The behaviour shown in figure 3 is typical. In all cases (squares excepted), we find that *the preferred mode* (according to linear theory) *is some number of finite rolls with axes parallel to the short side.*

The stability curves obtained have kinks which typify problems having independent stability curves. An example is the heating from below of an infinite rotating fluid layer where an overstability is possible (see Chandrasekhar 1961, p. 97, figure 21).

To see that our problem is inherently three-dimensional we need only note the following. If we view a two-dimensional channel as the limit of a three-dimensional box as, say, $h_2 \to \infty$, the critical Rayleigh number according to our results is attained with many finite y-rolls (for $h_1 = 1$, $R_c < 3500$ from figure 7). An analysis encompassing only two spatial dimensions, however, can describe only the most preferred number of (non-finite) x-rolls. Hence, Velte obtains $R_c = 5030$ for a single x-roll with $h_1 = 1$.

From figures 4–12, one can construct a map of the preferred mode according to linear theory (see figure 13). The figure is symmetric with respect to the line $h_1 = h_2$. The numbers appearing in the various zones denote the preferred number of finite rolls contained in the box. In addition, we have drawn curves of constant R_c.

One can illustrate the use of the diagram by following a solid vertical line at, say, $h_1 = 4$. On this line, $h_1 = 4$ and h_2 varies. When h_2 is small, many finite x-rolls are preferred, K decreasing to four as h_2 increases to the line $h_1 = h_2$.

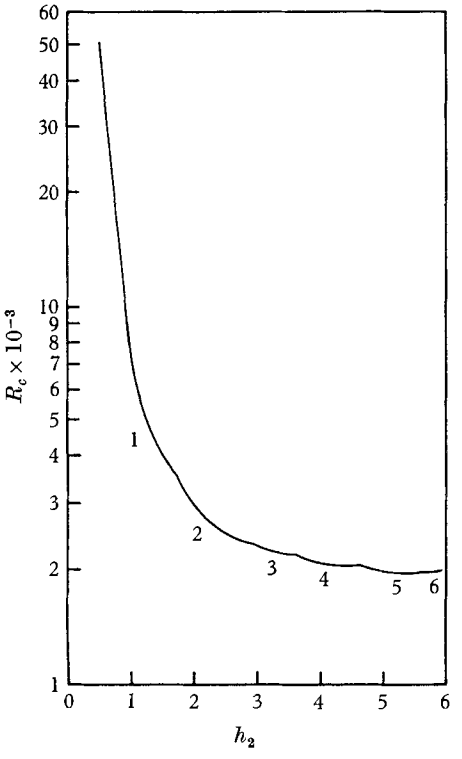

FIGURE 4

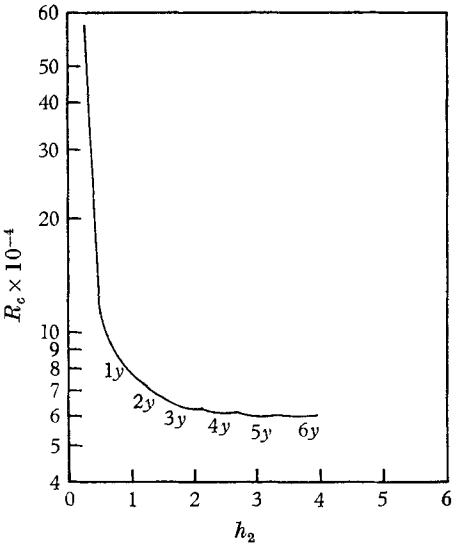

FIGURE 5

FIGURE 4. Stability curve for $h_1 = h_2$, any linear combination of n finite x-rolls and y-rolls allowed, n indicated. R_c versus h_2.

FIGURE 5. Stability curve for $h_1 = 0{\cdot}25$, n_x and m_y denote n finite x-rolls and m finite y-rolls respectively. R_c versus h_2.

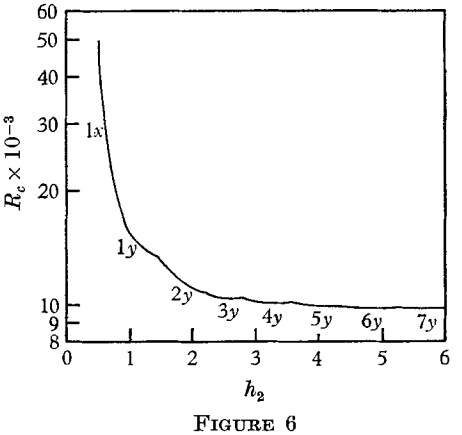

FIGURE 6

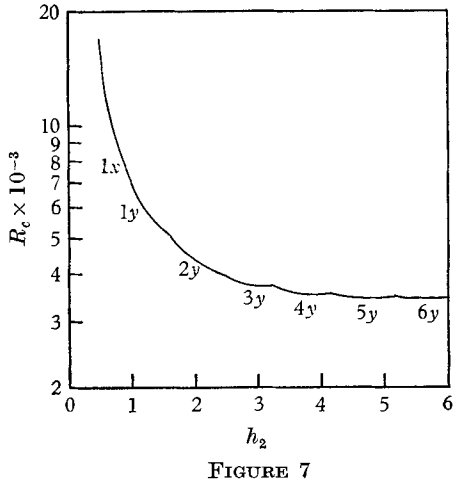

FIGURE 7

FIGURE 6. Stability curve for $h_1 = 0{\cdot}50$, n_x and m_y denote n finite x-rolls and m finite y-rolls respectively. R_c versus h_2.

FIGURE 7. Stability curve for $h_1 = 1{\cdot}0$, n_x and m_y denote n finite x-rolls and m finite y-rolls respectively. R_c versus h_2.

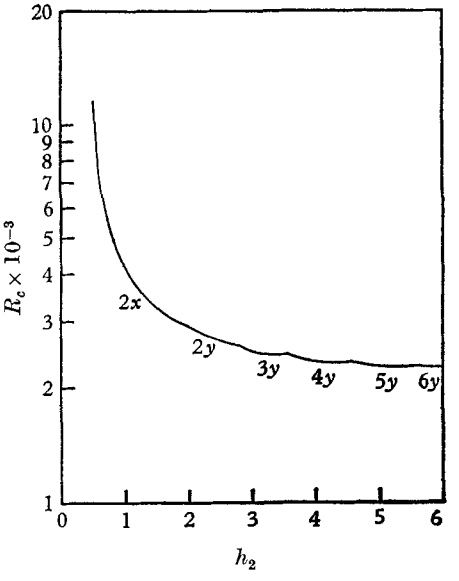

FIGURE 8

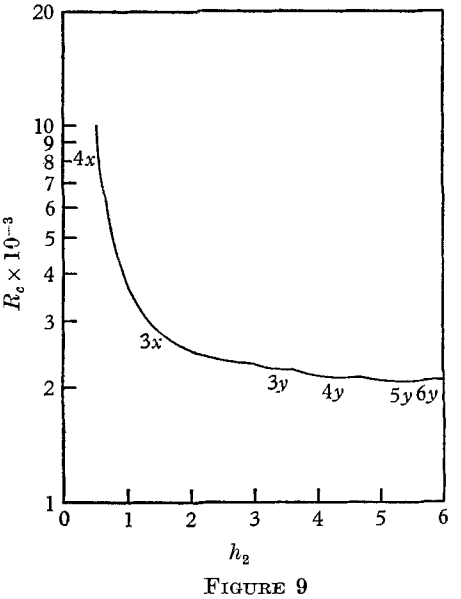

FIGURE 9

FIGURE 8. Stability curve for $h_1 = 2{\cdot}0$, n_x and m_y denote n finite x-rolls and m finite y-rolls respectively. R_c versus h_2.

FIGURE 9. Stability curve for $h_1 = 3{\cdot}0$, n_x and m_y denote n finite x-rolls and m finite y-rolls respectively. R_c versus h_2.

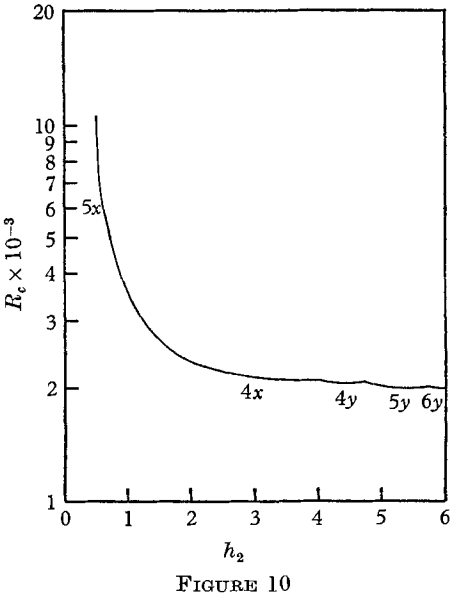

FIGURE 10

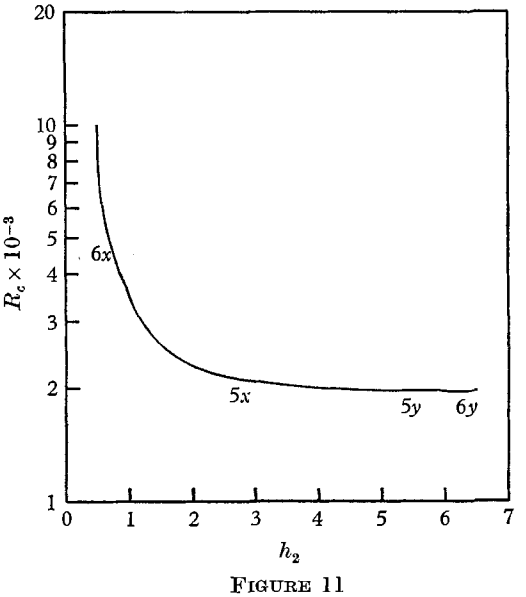

FIGURE 11

FIGURE 10. Stability curve for $h_1 = 4{\cdot}0$, n_x and m_y denote n finite x-rolls and m finite y-rolls respectively. R_c versus h_2.

FIGURE 11. Stability curve for $h_1 = 5{\cdot}0$, n_x and m_y denote n finite x-rolls and m finite y-rolls respectively. R_c versus h_2.

As we cross this line, four finite y-rolls become preferred. As h_2 increases further only finite y-rolls are preferred with K increasing without bound.

Koschmieder (1966) has remarked that 'rolls [form] parallel to the short side, so [that] they preferred the direction where they could develop in their usual height to diameter ratio 1:1', i.e. *rolls of square cross-section.* Figure 13 shows this to be the case *when the depth is the smallest dimension. Otherwise narrower cells are predicted.* (Koschmieder's h_1 and h_2 were of order 10.)

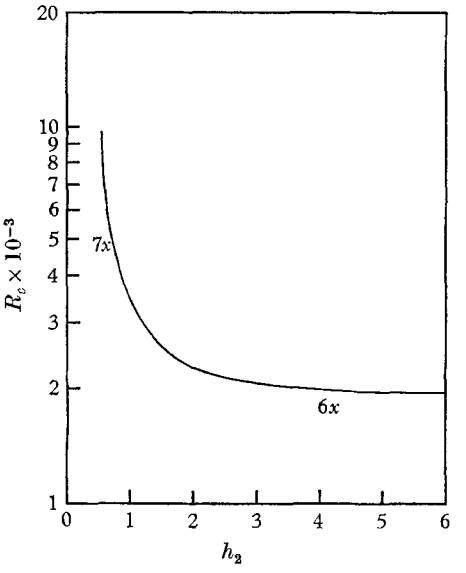

FIGURE 12

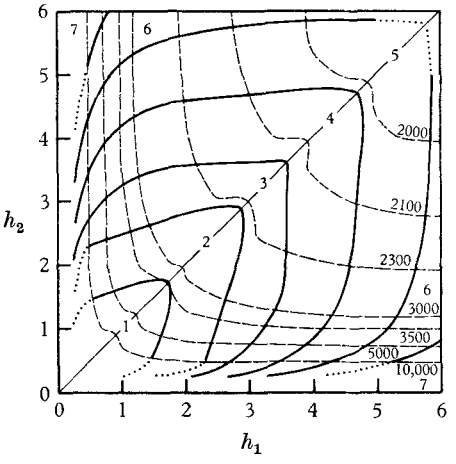

FIGURE 13

FIGURE 12. Stability curve for $h_1 = 6{\cdot}0$, n_x and m_y denote n finite x-rolls and m finite y-rolls respectively. R_c versus h_2.

FIGURE 13. Map of preferred wave-number (as indicated) of finite rolls as a function of h_1 and h_2. Dashed curves are of constant critical Rayleigh number. The figure is symmetric with respect to the line $h_1 = h_2$. Finite x-rolls are preferred below the line $h_1 = h_2$ and finite y-rolls above. Dotted lines are estimates of calculations which did not converge well numerically.

Another interesting fact can be observed in figure 13. When the long side of a box is increased beyond twice the other, subsequent increases do not affect R_c appreciably (although there are cell transitions). That is, a box whose lateral dimensions have a 2:1 ratio is effectively ∞:1 as far as the Rayleigh number is concerned (see comparison with work of Velte above).

5. Discussion

The inherently three-dimensional nature of the convection in a box gives rise to the two types of dependencies of R_c upon (h_1, h_2) for finite rolls as given in §3.

Type I occurs when a finite roll has its width varied and occurs for the same reasons as in the problem of an infinite layer. The critical Rayleigh number is attained as a compromise (Chandrasekhar 1961, p. 34) between the conflicting needs of viscous dissipation and release of potential energy. Narrow, tall cells

are inefficient because they dissipate large amounts of energy, while wide, flat cells are inefficient because a fluid particle must travel a great horizontal distance before it can fall and release its potential energy. Hence, we obtain a stability curve which has a finite minimum corresponding to moderate-sized cells being preferred.

Type II dependence is obtained when the length of a finite roll is varied. (This consideration is not present in the infinite layer where rolls have infinite length.) Since this variation does not materially change the length of the path of a fluid particle, the proximity of the walls at the 'ends' of the cell influence R_c mostly by affecting the viscous dissipation. The dissipation due to the end-walls is a small part of the total dissipation unless the finite roll is very short. The stability curve is a monotone decreasing function of the axial length of the finite roll and approaches a finite positive value of R_c rapidly.

In this study we have considered trial functions with two non-zero velocity components which represent finite rolls and have found that superpositions of these did not lower R_c or change the eigenfunction (within numerical accuracy). Let us consider physically the fact that a flow with only two non-zero velocity components in a three-dimensional domain seems to be preferred. At first glance one might consider the local behaviour of a finite roll near an end, as being similar to the situation of placing a rigid flat plate normal to the axis of a rotating flow (Bödewadt 1940). Bödewadt's problem, which yields an exact solution to the Navier–Stokes equations, illustrates the generation of a secondary axial flow which transforms the initially plane flow into a three-dimensional one. Two facts make the analogy with our problem inappropriate.

(i) The Bödewadt solution is a similarity solution of the *non-linear* equations of motion. The induced axial flow is a non-linear phenomenon.

(ii) The 'boundary-layer thickness' in the Bödewadt problem is $(\nu/\omega)^{\frac{1}{2}}$ where ν is the kinematic viscosity and ω is a local angular velocity. Even if we think of finite (but small) amplitude convection, the boundary layer will fill the whole box. Thus since the axial velocity must vanish at the end and $|\omega|$ is very small, the axial flow is very small. (Experiments seem to produce finite rolls.)

The *linear* stability problem considered in this paper is a slow flow whose correct local behaviour, near the end of a finite roll, can be modelled by a Stokes flow solution similar to that in Schmieden (1928), where the pressure is constant, the viscous forces are in balance, and the axial velocity is zero.

Thus the finite rolls approximate an exact solution which has a zero axial velocity or a negligibly small evenly distributed one. There are no sharp transition regions (boundary layers) near the ends. The speed of a particle approaches zero gradually as one nears an end.

When one solves the stability problem for a heated, infinite layer with the three sets of boundary conditions (1) free–free, (2) fixed–free, and (3) fixed–fixed, one notices that the preferred wavelength according to linear theory decreases from (1) to (2) to (3). The reason is that the more restrictive non-slip condition magnifies the viscous dissipation. For a convective cell to be sustained subject to this larger dissipation, a fluid particle must release its potential energy more efficiently. Hence, a narrower cell is predicted. In essence, our prediction of

finite rolls of cross-section smaller than square, when the depth is not the smallest dimension, has the same explanation. Consider finite x-rolls with h_1 fixed at, say, $h_1 = 2$. When $h_2 > 1$, cells of roughly square cross-section are preferred. When h_2 is decreased, however, the viscous dissipation at the ends becomes important and, in fact, for $h_2 < 1$, becomes the dominant portion. Convection is sustained only with more efficient potential energy release, i.e. narrower cells. This increased efficiency outweighs the increase in the dissipation due to narrowing, which is slight compared to that portion contributed at the ends. Thus we see that for, say $h_1 = 2$ and $h_2 \to 0$, more and more finite x-rolls tend to appear.

The basic assumptions in our analyses are that: (i) the walls are perfect heat conductors; (ii) the fluid properties are constants and the Boussinesq equations are valid.

Perfect heat conducting surfaces can be closely approximated in the laboratory although this condition does not describe well the conditions at the lateral walls of Koschmieder's apparatus.

Since the shape of the lateral walls of the box seem to determine the geometry of the convection cells in experiment, their influence is assumed to dominate over the small effects due to fluid property variations and 'non-Boussinesq-ness'. This assumption seems to be justified by our obtaining good agreement with the observations by Koschmieder.

When in figure 13 (h_1, h_2) lies on a stability boundary or on the line $h_1 = h_2$, linear theory predicts only an arbitrary linear combination of the relevant adjacent modes (those on either side of the curve). Finite amplitude effects must then determine the preferred mode.

The author wishes to express his gratitude to Dr Michael Sherman, Prof. R. S. Scorer, and Prof. J. T. Stuart for useful discussions and criticism and to Mr Richard Clasen and Mrs Margaret Ryan for invaluable aid with the numerical calculations. This work was supported by project RAND.

Appendix A. Computation of R_c

It can be shown that $R_c > 0$ for the infinite layer. Assume $R_c > 0$. Then the matrix

$$B = \begin{bmatrix} U & 0 \\ 0 & Z \end{bmatrix}$$

is non-singular and $$B^{-1} = \begin{bmatrix} U^{-1} & 0 \\ 0 & Z^{-1} \end{bmatrix}.$$

Therefore A is singular if and only if

$$B^{-1}A = \begin{bmatrix} U^{-1} & 0 \\ 0 & Z^{-1} \end{bmatrix} \begin{bmatrix} U & R^{\frac{1}{2}}V \\ R^{\frac{1}{2}}W & Z \end{bmatrix} = \begin{bmatrix} I_N & RU^{-1}V \\ R^{\frac{1}{2}}Z^{-1}W & I_N \end{bmatrix}$$

is singular where I_N is the $N \times N$ identity matrix. Also $B^{-1}A = I_{2N} - R^{\frac{1}{2}}C$ where

$$C = -\begin{bmatrix} 0 & U^{-1}V \\ Z^{-1}W & 0 \end{bmatrix}.$$

Hence A is a singular if and only if $R^{-\frac{1}{2}}$ is an eigenvalue of the matrix C, and R is finite and non-zero. Since C has an N-dimensional manifold of zero eigenvalues, R_c is obtained as the reciprocal of the largest eigenvalue of the matrix $Z^{-1}WU^{-1}V$. This is an N-dimensional problem rather than a $2N$-dimensional one and calculations can be done accurately.

Appendix B. Trial function

Trial functions for θ are taken of the form

$$\psi_n = \sum_{i=1}^{3} \sum_{j=1}^{J} g_{n,j}^{(i)} x_i^j,$$

where $(x_1, x_2, x_3) = (x, y, z)$, J is a fixed positive integer and the $\{g_{n,j}^{(i)}\}$ are real numbers. Similarly the $\boldsymbol{\phi}_n = (\phi_n^{(1)}, \phi_n^{(2)}, \phi_n^{(3)})$, the trial functions for $\mathbf{V}$, have the same form and additionally satisfy $\operatorname{div}\boldsymbol{\phi}_n = 0$. In both cases $\boldsymbol{\phi}_n$ and ψ_n vanish on all boundaries.

The above forms and restrictions give us great freedom in the choice of the coefficients so that we are able to approximate a configuration of, say, K finite x-rolls as follows:

(i) $\phi_n^{(1)} = 0$ at $(K-1)$ points of $\{x \mid |x| < \frac{1}{2}h_1\}$,

(ii) $\phi_n^{(2)} \equiv 0$,

(iii) $\phi_n^{(3)} \neq 0$ in $\{z \mid |z| < \frac{1}{2}\}$ (other dependences give higher Rayleigh numbers),

(iv) ψ_n has the same form as $\phi_n^{(3)}$ (but the condition $\partial\psi_n/\partial z = 0$ at $|z| = \frac{1}{2}$ is not required),

(v) all trial functions are even in y (other dependences give higher Rayleigh numbers).

REFERENCES

Bödewadt, U. T. 1940 *Zamm.* **20**, 241.

Chandrasekhar, S. 1961 *Hydrodynamic and Hydromagnetic Stability*. Oxford: Clarendon Press.

Davis, S. H. & Segel, L. A. 1965 *RAND Corporation Rept.* RM-4709, Santa Monica, California. (Submitted for publication.)

Koschmieder, E. L. 1966 *Beitr. Phys. Atmos.* **39**, 1.

Ostrach, S. & Pnueli, D. 1963 *ASME Transactions, Series C*, **85**, 346.

Pellew, A. & Southwell, R. V. 1940 *Proc. Roy. Soc.* A, **176**, 312.

Sani, R. L. 1963 Ph.D. Thesis, University of Minnesota, Department of Chemical Engineering.

Schlüter, A., Lortz, D. & Busse, F. 1965 *J. Fluid Mech.* **23**, 129.

Schmieden, C. 1928 *Zamm.* **8**, 460.

Segel, L. A. & Stuart, J. T. 1962 *J. Fluid Mech.* **13**, 289.

Velte, W. 1964 *Arch. Rat. Mech. Anal.* **16**, no. 2, 97.

Zierep, J. 1963 *Beitr. Phys. Atmos.* **36**, 70.